2.0 STRUCTURAL EVALUATION

This section presents evaluations demonstrating that the ATR FFSC package meets all applicable structural criteria. The ATR FFSC packaging, consisting of the body and closure, is evaluated and shown to provide adequate protection for each payload; the ATR fuel element, MIT fuel element, MURR fuel element, RINSC fuel element, or ATR loose fuel plates. Each fuel element is contained within a corresponding fuel handling enclosure (FHE). The loose fuel plate basket (LFPB) is evaluated to contain only loose fuel plates associated with the ATR fuel element.

Normal conditions of transport (NCT) and hypothetical accident condition (HAC) evaluations are performed to address 10 CFR §71[1] performance requirements primarily through physical testing. Physical demonstration by testing, including the free drop and puncture events, consists of certification testing utilizing two full-scale certification test units (CTU-1 and CTU-2). CTU-1 included the ATR fuel element payload and CTU-2 included the ATR LFPB and loose plates payload. Certification testing has demonstrated that the key performance objective of criticality control will be met by the ATR FFSC package. Details of the certification test program are provided in Appendix 2.12.1, *Certification Tests on CTU-1*, and Appendix 2.12.2, *Certification Tests on CTU-2*. The evaluation for the MIT and MURR fuel elements is provided in Appendix 2.12.3, *Structural Evaluation for MIT and MURR Fuel.*

2.1 Structural Design

2.1.1 Discussion

The ATR FFSC is a two part packaging consisting of the body and the closure. The body is a single weldment that features square tubing as an outer shell and round tubing for the payload cavity. The closure engages with the body using a bayonet style design. There are four lugs, uniformly spaced on the closure that engages with four slots in the mating body feature. The closure is secured by retracting two spring loaded pins, rotating the closure through approximately 45°, and releasing the spring loaded pins such that the pins engage with mating holes in the body. When the pins are properly engaged with the mating holes the closure is locked.

With the exception of several minor components, all steel used in the ATR FFSC packaging is of a Type 304 stainless steel. Components are joined using full-thickness fillet welds (i.e., fillet welds whose leg size is nominally equal to the lesser thickness of the parts joined) and full and partial penetration groove welds. The fuel containers for the package, the FHEs and the LFPB, are principally of aluminum construction and secured with stainless steel fasteners. The FHEs are a fabrication and the LFPB consists of four machined aluminum components.

A comprehensive discussion of the ATR FFSC packaging design and configuration is provided in Section 1.2, *Package Description.*

[1] Title 10, Code of Federal Regulations, Part 71 (10 CFR §71), *Packaging and Transportation of Radioactive Material*, 01-01-06 Edition.

2.1.2 Design Criteria

The ATR FFSC package has been designed to meet the majority of applicable structural requirements of 10 CFR §71 through physical testing. The design objectives for the package are threefold:

1. For NCT, demonstrate that the ATR FFSC package contains the payload without dispersal and that it does not experience a significant reduction in its effectiveness to withstand HAC; and
2. For HAC, demonstrate that the ATR FFSC package contains the payload without dispersal, consistent with conservative bounding assumptions utilized in the criticality analysis.
3. For HAC, demonstrate that the insulation used in the ATR FFSC package remains in place, to protect the payload from excessive heat from the thermal test, within the assumptions utilized in the thermal analysis.

Consequently, the design criteria for NCT are that the ATR FFSC package exhibit only minor damage subsequent to the NCT conditions and tests, including no damage that would materially affect the outcome of the subsequent HAC tests.

For HAC, the design criteria is that the payload will be retained within the packaging subsequent to the HAC test series of free drop, puncture, thermal, and the immersion test of 10 CFR §71.73(c)(5), or subsequent to immersion of an undamaged specimen per 10 CFR §71.73(c)(6).

Material properties are controlled by the acquisition of critical components to ASTM standards, testing, and process control, as described in Section 2.2, *Materials*. Lifting devices that are a structural part of the package are designed with a minimum safety factor of three against yielding. The index lugs located at the top of the package are considered a tiedown devices and are designed to withstand the loading requirements per 10 CFR §71.45(b)(1).

2.1.2.1 Miscellaneous Structural Failure Modes

2.1.2.1.1 Brittle Fracture Assessment

The steel materials utilized in the ATR FFSC package provide adequate fracture toughness. All critical structural components of the packaging are made of Type 304 stainless steel and have a nil ductility transition temperature less than -40°F (-40°C). Therefore, brittle fracture is not a concern for the ATR FFSC packaging.

To confirm the performance of the uranium aluminide (UAl_x) fuel types at reduced temperatures, the ATR fuel element in CTU-1, was subjected to two HAC drops with the payload at approximately -20°F (-29°C). Following all CTU-1 testing, as discussed in Appendix 2.12.1, *Certification Tests on CTU-1*, the package was disassembled and the payload inspected. Upon inspection, the performance of both the payload and packaging, including the reduced temperature tests, was satisfactory. Following all testing, the payload remained within the assumptions presented in Section 6.0, *Criticality Evaluation*.

2.1.2.1.2 Fatigue Assessment

Normal operating cycles do not present a fatigue concern for the ATR FFSC. The packaging does not retain pressure, and consequently fatigue due to pressure cycling cannot occur. Since all structural components of the packaging are made of the same alloy, and since thermal gradients are small, thermally-induced fatigue is not of concern. Since the packaging is normally handled on a pallet, the lifting features of the packaging are infrequently used, and fatigue of the lifting load path is not of concern.

The only components which are routinely handled are the closure and the fuel handling structures (ATR, MIT, MURR, and RINSC fuel handling enclosures and loose plate basket). The closure is designed as a bayonet-type attachment with two spring-loaded locking pins which prevent rotation during transport. Neither the bayonet lugs nor the locking pins experience any significant loading (such as preload or other repeating mechanical loads) in routine usage. If damage to these components were to occur, it will be identified during the inspections discussed in Section 7.1.1, *Preparation for Loading*. Consequently, fatigue of the closure components is not of concern.

The fuel handling structures (fuel handling enclosures and loose plate basket) are simple structures that do not have significant handling loads. These structures are fully exposed to view during loading and unloading, and can be inspected to ensure integrity.

For these reasons, normal operating cycles are not a failure mode of concern for the ATR FFSC packaging. Fatigue associated with normal vibration over the road is discussed in Section 2.6.5, *Vibration.*

2.1.2.1.3 Buckling Assessment

Certification testing has demonstrated that buckling of the ATR FFSC package does not occur as a result of any normal conditions of transport or as a result of the HAC primary test sequence (e.g., the free drop and puncture tests). Buckling of the ATR FFSC body is also shown to not be a concern during the 50 ft immersion test specified under 10 CFR §71.73(c)(6). A discussion of the response to the 50 ft immersion test is provided in Section 2.7.6, *Immersion – All Packages.*

2.1.3 Weights and Centers of Gravity

The maximum gross weight of the ATR FFSC package is 290 lb. The packaging component weights are summarized in Table 2.1-1. The maximum payload weight is 50 lb, for the loose plate payload, 40 lb for the ATR payload, 35 lb for the MIT payload, 45 lb for the MURR payload, and 45 lb for the RINSC payload. Due to symmetry of design, the center of gravity (CG) of the package is located essentially at the geometric center of the package. Regardless of payload, the center of gravity remains 35 inches from the face of the closure end and 4 inches from the bottom and sides of the package. The packaging components are illustrated in Figure 2.1-1 through Figure 2.1-5.

Table 2.1-1 – ATR FFSC Component Weights

Item	Weight, lb	
	Component	Assembly
ATR FFSC Packaging	- -	240
Body Assembly	230	- -
Closure Assembly	10	- -
Payload – ATR Fuel Assembly	- -	40
ATR Fuel Assembly	25	- -
ATR Fuel Handling Enclosure	15	- -
Payload – MIT Fuel Assembly	- -	35
MIT Fuel Assembly	10	- -
MIT Fuel Handling Enclosure	25	- -
Payload – MURR Fuel Assembly	- -	45
MURR Fuel Assembly	15	- -
MURR Fuel Handling Enclosure	30	- -
Payload – RINSC Fuel Assembly	- -	45
RINSC Fuel Assembly	17	- -
RINSC Fuel Handling Enclosure	28	- -
Payload – Fuel Plates	- -	50
ATR Loose Fuel Plates (including optional dunnage)	20	- -
Loose Fuel Plate Basket	30	- -
Total LFPB Loaded Package (maximum)	- -	290
Total MURR Loaded Package	- -	285
Total ATR Loaded Package	- -	280
Total MIT Loaded Package	- -	275
Total RINSC Loaded Package	- -	275

2.1.4 Identification of Codes and Standards for Package Design

As a Type AF package, the ATR FFSC is designed to meet the performance requirements of 10 CFR 71, Subpart E. Compliance with these requirements is demonstrated via full scale testing of the package under both NCT and HAC, as documented in Section 2.12, *Appendices*. In addition, structural materials which are important to safety are specified using American Society for Testing and Materials (ASTM) standards as shown on the drawings in Appendix 1.3.2, *Packaging General Arrangement Drawings*. Welding procedures and personnel are qualified in accordance with the ASME Code, Section IX. All welds are visually examined on each pass per the requirements of AWS D1.6:1999[2] for stainless steel and AWS D1.2:2003[3] for

[2] ANSI/AWS D1.6:1999, *Structural Welding Code – Stainless Steel*, American Welding Society (AWS).

[3] ANSI/AWS D1.2:2003, *Structural Welding Code – Aluminum*, American Welding Society (AWS)

aluminum. All welds which are important to safety are examined by liquid penetrant test on the final pass using procedures compliant with ASTM E165-02[4].

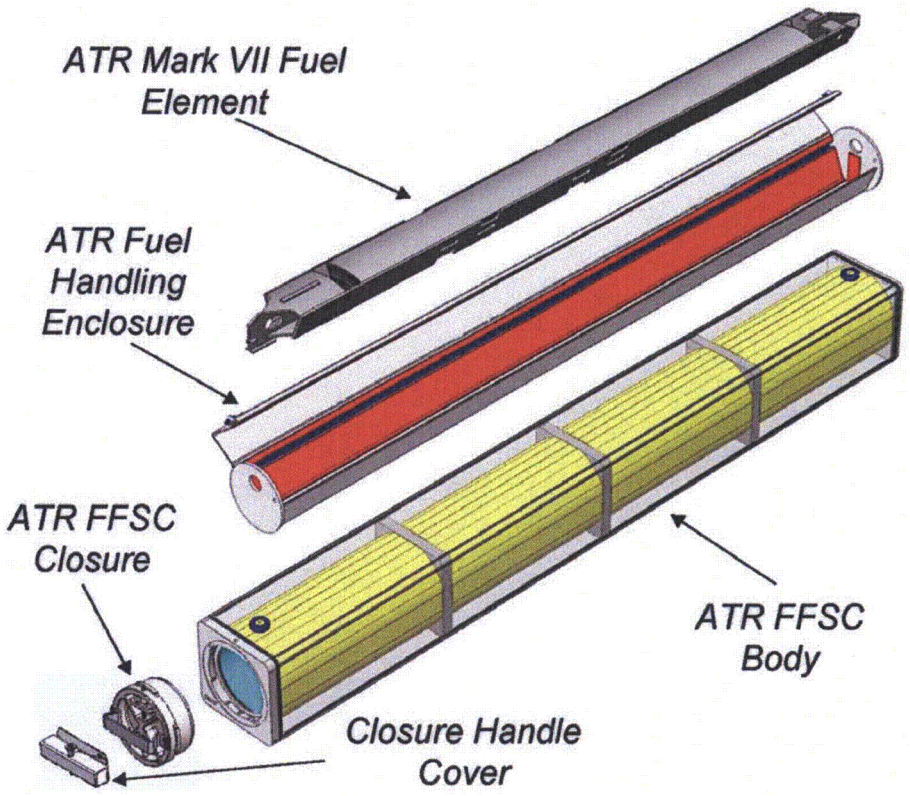

Figure 2.1-1 –Package Components (With ATR Fuel Element)

[4] American Society for Testing and Materials (ASTM International), ASTM E165-02, *Standard Test Method for Liquid Penetrant Examination*, Feb 2002.

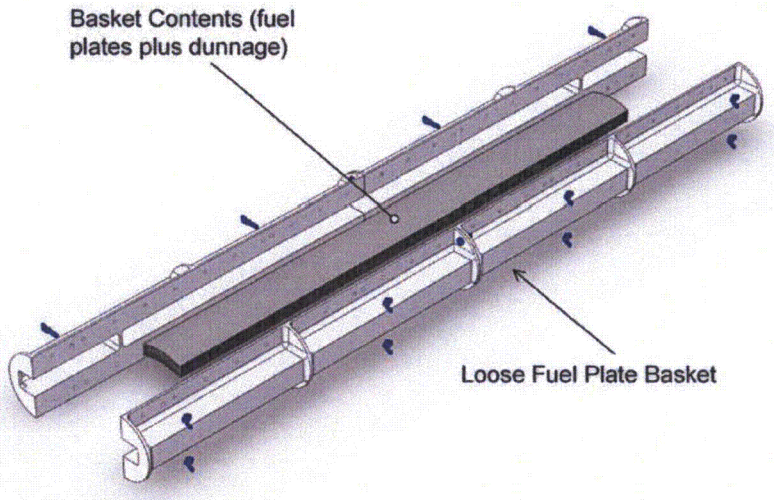

Figure 2.1-2 –Loose Fuel Plate Basket Components

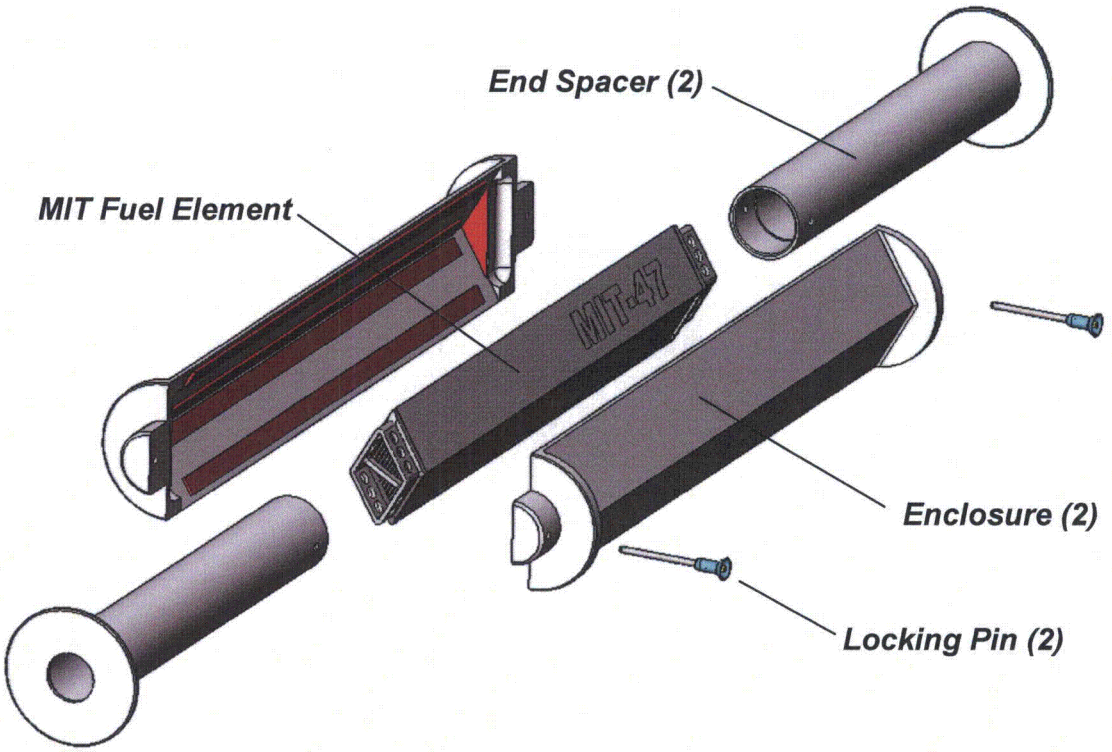

Figure 2.1-3 – MIT Fuel Handling Enclosure

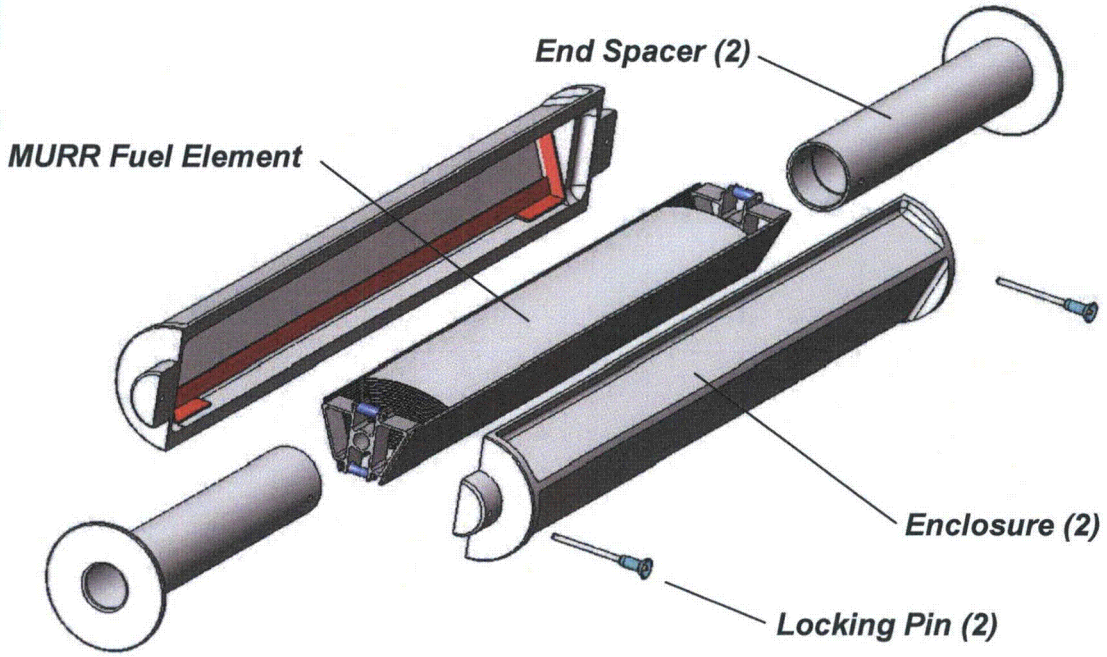

Figure 2.1-4 – MURR Fuel Handling Enclosure

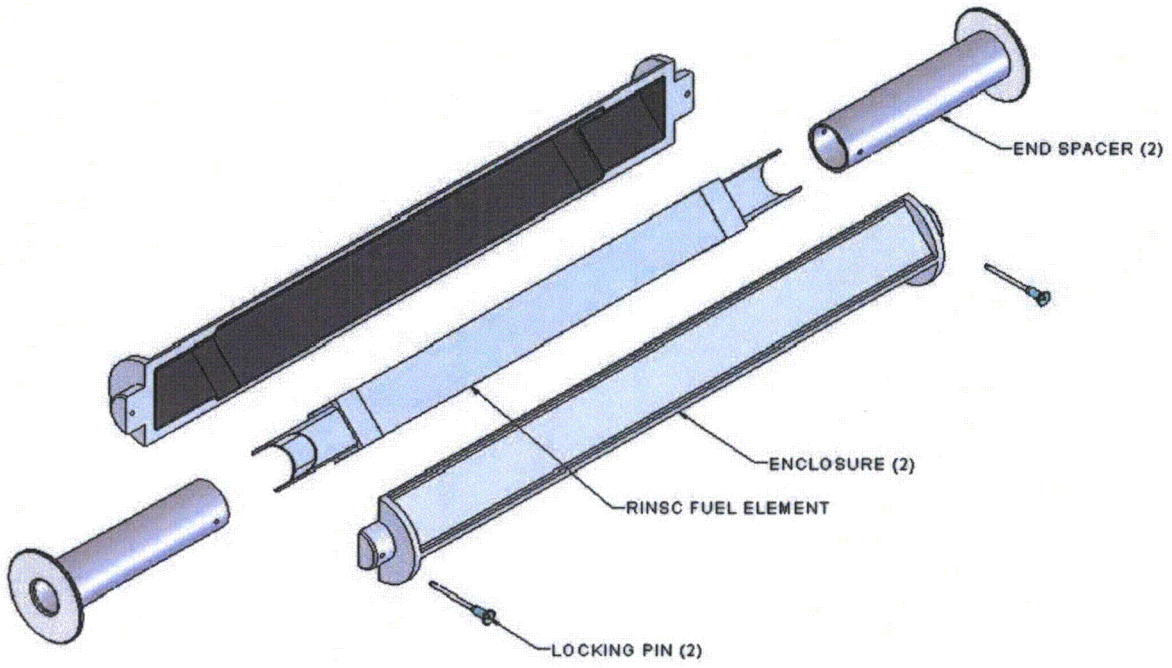

Figure 2.1-5 – RINSC Fuel Handling Enclosure

2.2 Materials

The ATR FFSC package is constructed primarily from Type 304 stainless steel structural materials. The drawings presented in Appendix 1.3.1, *Packaging General Arrangement Drawings*, delineate the specific materials used for each ATR FFSC packaging components.

2.2.1 Mechanical Properties and Specifications

Since the demonstration of compliance with the regulations is primarily via performance testing of full-scale prototypes, analytical structural evaluations are in general not performed. Properties of structural materials are controlled either by purchase to an ASTM or other standard or via a written specification.

2.2.1.1 Stainless Steel

All of the structural steel used in the ATR FFSC packaging is an ASTM grade stainless steel. The weld consumable material is ASTM Type 308-308L, which results in weld metal deposits which have properties at least as great as the base metal. The minimum properties of the stainless steel items are given in Table 2.2-1.

Table 2.2-1 –Material Properties of Stainless Steel

Material	Yield Strength, minimum, psi	Ultimate Strength, minimum, psi
ASTM A240 Type 304	30,000	75,000
ASTM A269 Type 304	30,000	75,000
ASTM A276 Type S21800	50,000	95,000
ASTM A479 Type 304	30,000	75,000
ASTM A554 Grade MT-304	30,000	75,000

2.2.1.2 Aluminum

The internal FHEs and LFPB are fabricated from aluminum alloy. Minimum material properties are given in Table 2.2-2.

Table 2.2-2 –Material Properties of Aluminum

Material	Yield Strength, minimum, psi	Ultimate Strength, minimum, psi
ASTM B209, Alloy 5052 – H32	23,000	31,000
ASTM B209, Alloy 6061 – T651 or 6061 – T6511, 4" Plate	35,000	40,000
ASTM B210, Alloy 6061 – T6 ¼" Thick	35,000	42,000
ASTM B211, Alloy 6061 – T651 or 6061 – T6511	35,000	42,000
ASTM B221 or B241, Alloy 6061 – T651 or 6061 – T6511	35,000	38,000

2.2.2 Chemical, Galvanic, or Other Reactions

The materials of construction of the ATR FFSC packaging are primarily Type 304 stainless steel and refractory insulation. Since these materials are relatively unreactive, no excessive corrosion or other reactions will occur during normal use. The package is normally transported in a closed van, and is not subject to immersion or exposure to water or chemicals other than occasional precipitation or mild cleaning agents. In addition, all of these materials have been used in Type A and Type B packagings for many years without incident. If unusual corrosion of the stainless steel components occurs, it can be readily detected during preparation of the packaging for use. The refractory insulation is sealed within the body and is not subject to chemical degradation or corrosion during normal use.

The payloads, consisting of either the FHE and corresponding fuel element or the LFPB and fuel plates, are constructed primarily of aluminum alloy. There is no galvanic or other reactions between the stainless steel package and aluminum alloy payload. Furthermore, the FHEs and LFPB are inspected prior to placement within the packaging.

2.2.3 Effects of Radiation on Materials

Since the payload of the ATR FFSC consists of contact handled un-irradiated fuel elements (or loose fuel plates), enriched to a maximum of 94% U-235, the radiation from the payload is insignificant. Consequently, there will be no radiation effects on the materials of construction and the requirements of 10 CFR §71.43(d) are met.

2.3 Fabrication and Examination

2.3.1 Fabrication

The metallic components of the ATR FFSC packaging are fabricated using conventional metal forming and welding techniques. Structural materials which are important to safety are specified using American Society for Testing and Materials (ASTM) standards as shown on the drawings in Appendix 1.3.2, *Packaging General Arrangement Drawings*. All materials and components are procured and assembled under a 10 CFR 71, Subpart H quality assurance program. Welding procedures and personnel are qualified in accordance with the ASME Code, Section IX. Each packaging and its components are fabricated in accordance with the requirements delineated on the drawings in Appendix 1.3.2, *Packaging General Arrangement Drawings*.

2.3.2 Examination

Each packaging and its components are examined per the requirements delineated on the drawings in Appendix 1.3.2, *Packaging General Arrangement Drawings*. All welds are visually examined on each pass per the requirements of AWS D1.6:1999 for stainless steel and AWS D1.2:2003 for aluminum. All welds which are important to safety are examined by liquid penetrant test on the final pass using procedures compliant with ASTM E165-02. Personnel performing NDE shall be qualified in accordance with ASNT SNT-TC-1A[5]. Any deviations from SAR drawing requirements will be dispositioned and corrected under a 10 CFR 71, Subpart H quality assurance program prior to the application of the model number, per 10 CFR §71.85(c).

2.4 General Requirements for All Packages

This section defines the general standards for all packages. The ATR FFSC package meets all requirements of this section.

2.4.1 Minimum Package Size

The minimum dimension of the ATR FFSC package is 8 inches square. Thus, the 4 inch minimum requirement of 10 CFR §71.43(a) is satisfied.

2.4.2 Tamper-Indicating Feature

A tamper-indicating device (TID) lock wire and seal is installed through a small post on the closure provided to receive the wire. An identical post is located on the body for the TID wire. For ease in operation, there are two TID posts on the body. There are only two possible angular orientations for the closure installation and the duplicate TID post on the body enables TID installation in both positions. Thus, the requirement of 10 CFR §71.43(b) is satisfied.

[5] American Society for Nondestructive Testing (ASNT), Recommended Practice No. ASNT SNT-TC-1A, 2001 Edition.

2.4.3 Positive Closure

The ATR FFSC package cannot be opened unintentionally. The closure engages with the body using a bayonet style design. There are four lugs, uniformly spaced on the closure, that engage with four slots in the mating body feature. The closure is secured by retracting two spring loaded pins, rotating the closure through approximately 45°, and releasing the spring loaded pins such that the pins engage with mating holes in the body. When the pins are properly engaged with the mating holes the closure is locked. Thus, the requirements of 10 CFR §71.43(c) are satisfied.

2.4.4 Valves

The ATR FFSC does not contain any valves.

2.4.5 External Temperatures

As discussed in Section 3.3.1.1, *Maximum Temperatures*, the maximum accessible surface temperature with no insolation is 100°F (38°C). Since the maximum external temperature does not exceed 122°F (50°C), the requirements of 10 CFR §71.43(g) are satisfied.

2.5 Lifting and Tiedown Standards for All Packages

2.5.1 Lifting Devices

The ATR FFSC package may be lifted from beneath utilizing a standard forklift truck when the package is secured to a fork pocket equipped pallet, or in a package rack. Swivel lift eyes can be installed in the package to enable package handling with overhead lifting equipment. The swivel eyes are installed after removing the 3/8-16 socket flat head cap screws and index lugs used for stacking.

Assuming both lift eyes carry half the load, the weight at each lug is:

$$P = (\frac{290}{2}) = 145\ lbf$$

Applying a minimum horizontal sling angle of 30°, the maximum load on each sling is:

$$T = \frac{145}{\sin(30)} = 290\ lbf$$

Therefore, all lifting devices shall have a minimum working load limit of 300 lb.

2.5.1.1 Attachment Capacity

Per 10 CFR §71.45(a) any lifting attachment that is a structural part of the package must be designed with a minimum safety factor of three against yielding. This evaluation verifies the adequacy of the groove weld securing the threaded bar to the wall of the 8 inch square tube. By inspection, the groove weld is the weakest point of the lifting point and all other items will have

a greater margin of safety. The lift eye is required to have a minimum working load limit of 300 lb. The lift eye components are therefore assumed to meet the lifting requirements.

The allowable force on the groove weld is equal to the shear strength of the base material, $0.6*\sigma_{yield}$.

Allowable weld stresses:

$$\sigma_{yield} = 30{,}000\ psi$$

$$w_{allow} = 0.6 \cdot 30{,}000 = 18{,}000\ psi$$

Maximum tension in each of the two lift slings is 290 lbf at an angle of 30°.

$$T_y = P = 145\,lbf$$

$$T_x = 290 \cdot \cos(30) = 251\,lbf$$

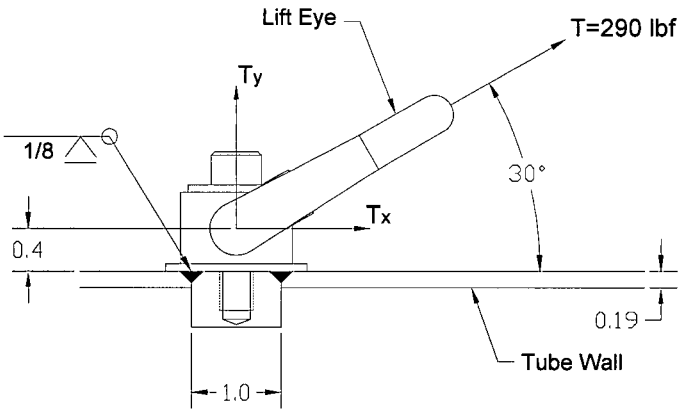

Figure 2.5-1 – Lift Attachment Diagram

Including the safety factor of three, the maximum horizontal and vertical forces are:

$$P_h = 3 \cdot T_x = 753\,lbf$$

$$P_v = 3 \cdot T_y = 435\,lbf$$

Using Blodgett[6], the given load is divided by the length of the weld to arrive at the applied unit force, lb per linear inch of weld. From this force, the proper throat of the grove weld is determined.

The properties of the weld, treated as a line, are:

[6] Omer Blodgett, *Design of Welded Structures*, 1982, The James F. Lincoln Arc Welding Foundation, Cleveland, Ohio.

$$A_w = \pi \cdot d$$

$$S_w = \frac{\pi \cdot d^2}{4}$$

Where,

d = diameter of weld = 1.0 inch

$$A_w = \pi \cdot (1) = 3.14\,in$$

$$S_w = \frac{\pi \cdot (1)^2}{4} = 0.785\,in^2$$

Vertical tension on the weld is:

$$f_v = \frac{P_v}{A_w} = \frac{435}{3.14} = 139\,\frac{lbf}{in}$$

Horizontal shear on the weld is:

$$f_h = \frac{P_h}{A_w} = \frac{753}{3.14} = 240\,\frac{lbf}{in}$$

The bending force on the weld is

h = height of applied load from lift eye = 0.4 in, plus half of the weld thickness of 0.125/2

$$h = 0.4 + (.125/2) = 0.463\,in$$

$$M = P_h \cdot h = 753 \cdot 0.463 = 349\,in \cdot lb$$

$$f_b = \frac{M}{S_w} = \frac{349}{0.785} = 445\,\frac{lbf}{in}$$

The vertical tension and bending forces are in the same direction and additive:

$$f_{v+b} = f_v + f_b = 139 + 445 = 584\,\frac{lbf}{in}$$

The vertical and horizontal loads are perpendicular, therefore the combined load is:

$$f_r = \sqrt{(f_{v+b})^2 + f_h^{\,2}} = \sqrt{(584)^2 + (240)^2} = 631\,\frac{lbf}{in}$$

The required grove weld is:

$$w = \frac{f_r}{w_{allow}} = \frac{631}{18{,}000} = 0.035\,in$$

Thus the weld margin of safety is:

$$MS_{weld} = \frac{.125}{.035} - 1 = +2.6$$

2.5.1.2 Conclusion

From the above analyses, the lifting attachment points adequately lift the fully loaded package with a margin of safety of 2.6. The conservative minimum lifting angle of the slings is 30° above horizontal. Failure of this lifting component under excessive load would not impair the ability of this package to meet other requirements of 10 CFR §71, per the requirements of 10 CFR §71.45(a).

2.5.2 Tiedown Devices

For transport, the package will be strapped or otherwise restrained inside or on the transport vehicle. Any features used to lift the ATR FFSC will be removed or rendered unusable for tiedown. The index lugs used to align the package during stacking are evaluated for the tiedown loads. Per 10 CFR §71.45(b)(1) the tiedown system must withstand a vertical loading of 2g, horizontal for/aft loading of 10g, and horizontal lateral loading of 5g. Because there is no vertical restraint capability of the index lug, the 2g vertical load is neglected. Combining the loads, the maximum horizontal g loading is $\sqrt{10^2 + 5^2} = 11.18g$. The loaded ATR FFSC package weighs 290 lb.

2.5.2.1 Tiedown Method

The ATR FFSC may be stacked in a 4 wide by 3 high array during transport. The packages are secured by means which resist the vertical loading. However, any axial/lateral restraint is conservatively neglected.

The index lugs at each end of the packages are used to align and secure the packages within the array and are subjected to g-loads from neighboring packages. The index lugs are attached to the package by a single flat head, socket cap screw such that horizontal loading causes shearing in the threaded area of the screw as shown in Figure 2.5-2.

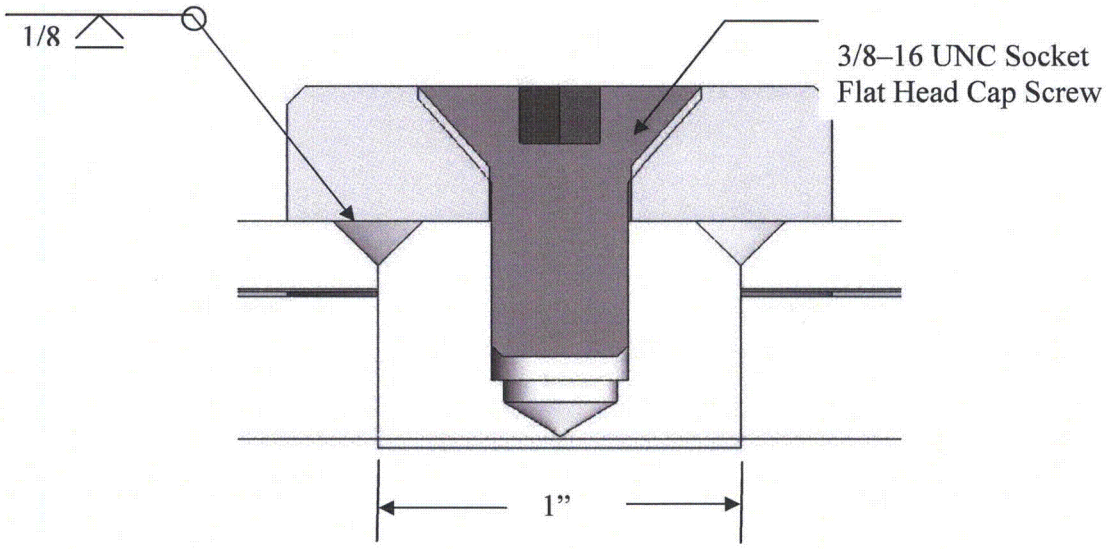

Figure 2.5-2 – Index Lug

2.5.2.2 Tiedown Capacity

By assuming the package is not restrained horizontally, the index lugs of the first tier must resist the horizontal loading of the middle and top tiers. The maximum load on each button is 2W times the g loading.

$$P_h = \frac{(2)(290)(11.18)}{2} = 3{,}242 \ lbf$$

2.5.2.3 Fasteners

The screw thread shear area is 0.0775 in^2 and the screw material is ASTM F835 which has minimum tensile strength of 145 ksi. The yield strength is 116 ksi; conservatively assuming yield to be 80% of tensile strength for alloy steel. The shear force allowable is $0.6\sigma_{yield}$.

$$\text{Fastener shear stress} = \frac{3{,}242}{0.0775} = 41{,}832 \ psi$$

$$MS = \frac{(116{,}000)(.6)}{41{,}832} - 1 = +0.66$$

The load required to fail the screw is:

$$P_{h-failure} = 0.6 \cdot \sigma_{ult} \cdot A = (0.6 \cdot 145{,}000) \cdot (0.0775) = 6{,}743 \ lbf$$

2.5.2.4 Weld Structure

The allowable force on the groove weld is equal to the shear strength of the base material, $0.6\sigma_{yield}$.

Allowable weld stresses:

$$\sigma_{yield} = 30{,}000 \ psi$$

$$w_{allow} = 0.6 \cdot 30{,}000 = 18{,}000 \ psi$$

Using Blodgett, the given load is divided by the length of the weld to arrive at the applied unit force, lb per linear inch of weld. From this force, the proper throat of the grove weld is determined.

The properties of the weld, treated as a line, are:

$$A_w = \pi \cdot d$$

$$S_w = \frac{\pi \cdot d^2}{4}$$

Where,

d = diameter of weld = 1.0 inch

$$A_w = \pi \cdot (1) = 3.14 \ in$$

$$S_w = \frac{\pi \cdot (1)^2}{4} = 0.785 \ in^2$$

Horizontal shear on the weld is:

$$f_h = \frac{P_h}{A_w} = \frac{3{,}242}{3.14} = 1{,}033\ lbf/in$$

Assume for simplicity that the index lug diameter matches that of the weld (conservative). The moment on the weld is equal to the applied load times the distance from the weld c.g. to the mid-height of the 3/8 inch high index lug, or:

$$\frac{0.125}{2} + \frac{0.375}{2} = 0.25\ in$$

The bending force on the weld, as a vertical component, is

h = height of applied load to index lug = 0.25 in

$$M = P_h \cdot h = 3{,}242 \cdot 0.25 = 811\ in \cdot lb$$

$$f_b = \frac{M}{S_w} = \frac{811}{0.785} = 1{,}033\ lbf/in$$

The vertical and horizontal loads are perpendicular, therefore the combined load is:

$$f_r = \sqrt{f_b^{\,2} + f_h^{\,2}} = \sqrt{(1{,}033)^2 + (1{,}033)^2} = 1{,}461\ lbf/in$$

The required grove weld is:

$$w = \frac{f_r}{w_{allow}} = \frac{1{,}461}{18{,}000} = .081\ in$$

Thus the weld margin of safety is:

$$MS_{weld} = \frac{.125}{.081} - 1 = +0.54$$

The load required to fail the weld is:

$$f_r = w \cdot (0.6 \cdot w_{ult}) = (0.125) \cdot (0.6 \cdot 75{,}000) = 5{,}625\ lbf/in$$

Since $f_b = f_h$: $f_h = \sqrt{f_r^{\,2}/2} = \sqrt{(5{,}625)^2/2} = 3{,}977\ lbf/in$

The load required to fail the weld is:

$$P_{h-failure} = f_h \cdot A_w = (3{,}977) \cdot (3.14) = 12{,}488\ lbf$$

2.5.2.5 Conclusion

From the above analysis, the index lugs adequately withstand the combined horizontal tiedown g-loads for the fully loaded package. Furthermore, it is shown that the index lug screw will fail prior to the weld. This satisfies the requirements of 10 CFR §71.45(b)(1).

2.5.3 Closure Handle

The closure handle, deemed a structural part of the package, must be rendered inoperable for lifting and tiedown during transport in compliance with 10 CFR §71.45. To satisfy this requirement, a cover will be secured over the closure handle during transport to prevent any straps or hooks from being attached to the handle or to prevent any hardware from being placed between the handle and closure as illustrated in Figure 1.2-5. As an option, the handle may also be removed during transport.

The attachment of the closure handle to the closure assembly is evaluated here to show that its failure will not impair the ability of the package to meet other requirements. A lifting or tiedown load applied to the closure handle is expected to deform the handle and fail the closure screws causing the handle to become detached from the closure assembly. The closure handle is used only for operator convenience in handling the 10 lb closure assembly by hand. The four small fasteners securing the handle to the closure are designed to fail under light loads and well before impairment of any safety related packaging feature.

This evaluation conservatively neglects any tension (pulling) on the handle and handle screws since a load in this direction would pull on the closure locking tabs and not the locking pins. A simple comparison between the area of the closure tabs and the area of the handle screws shows that the closure tabs consist of significantly more material and the screws will fail well before any significant loads are applied to the closure tabs.

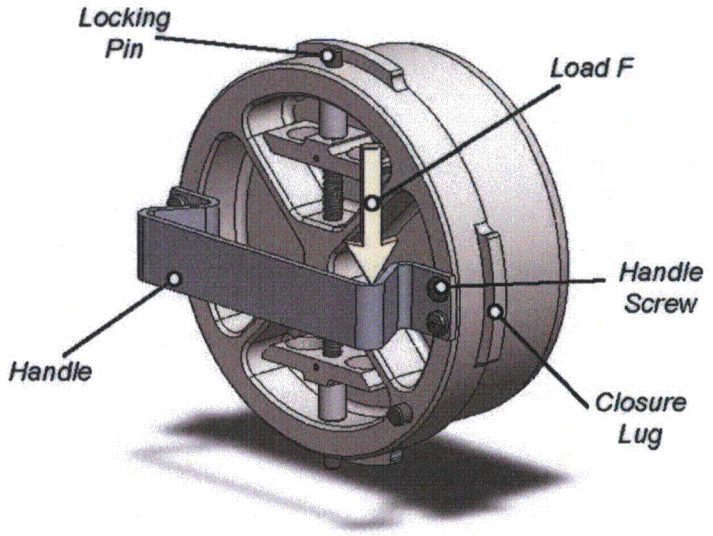

Figure 2.5-3 – Closure Assembly Handle

2.5.3.1 Handle Fasteners

The closure handle is secured by four #10-24 UNC screws (two per side). For this evaluation the load F is applied at the outside edge of the handle: 0.5 inches radially out from the screws and 0.5 inches above the face of the closure assembly.

This evaluation is based on the load F necessary to fail the handle screws. The load will be a function of the ultimate strength of the handle screws, which are given as a minimum of 72,000 psi for 18-8 material. To account for possible strain hardening due to the manufacturing process, that value will be conservatively multiplied by a factor of 2. Therefore:

$$\sigma_{ultimate} = 144{,}000 \text{ psi}$$

For the handle screws, the area across the threads is equal to the area of the minor diameter. For a #10-24UNC screw the minor diameter is 0.1389 inches.

$$A_s = \frac{\pi d_m^{\ 2}}{4} = \frac{\pi (0.1389)^2}{4} = 0.0152 \text{ in}^2$$

The shear force in each screw is now determined. The largest forces will be at the two screws closest to the applied force. See Figure 2.5-4.

$$M = F \cdot r = 3.25\ F\ in \cdot lb$$

$$r = 3.25\ in\ (dist.to\ centroid)$$

Where r is taken as the maximum distance possible for any handle configuration.

The primary shear is:

$$n = 4 \text{ (number of screws)}$$

$$S' = \frac{F}{n} = \frac{F}{4} = 0.25F \text{ lb}$$

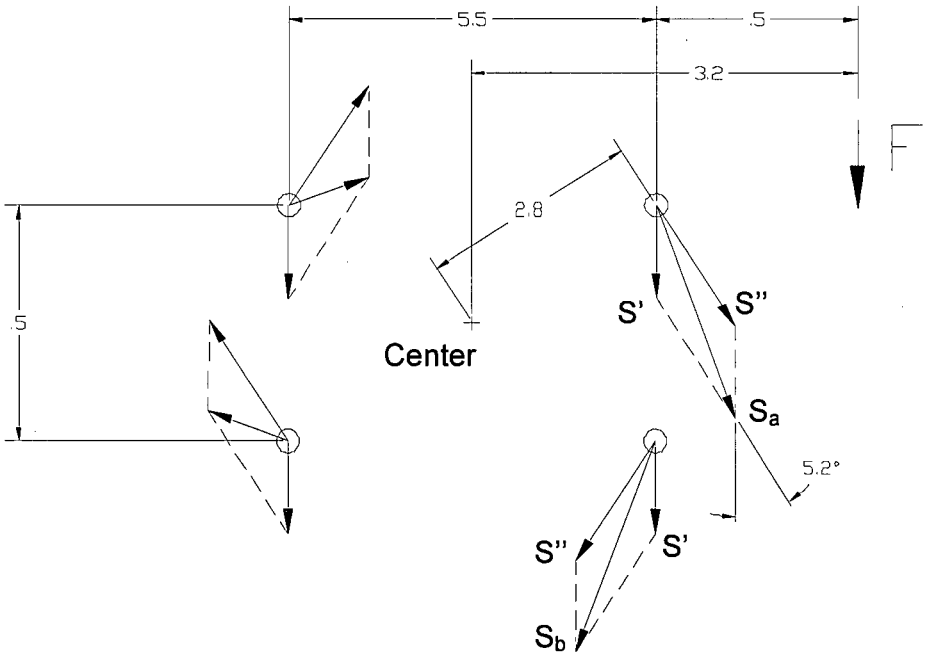

Figure 2.5-4 – Screw Pattern Diagram

The secondary shear is:

$$S'' = \frac{M}{4 \cdot R} = \frac{3.25F}{4 \cdot 2.8} = 0.29F \text{ lb}$$

$R = 2.8$ in. (dist. to centroid)

The combined shear force is:

$$S_a = S_b = 0.29F + 0.25F(\cos 5.2) = 0.29F + 0.249F = 0.539F$$

The shear stress is:

$$\tau = \frac{S_a}{A_s} = \frac{0.539F}{0.0152} = 35.46F \text{ psi}$$

The tensile load on the screws due to the load F is applied to only two of the four screws, since the handle, due to its flexibility, cannot effectively transfer the load to the screws on the opposite side of the handle. The tensile load on the two screws closest to the load is:

$$\sum M_A = F \cdot (0.5) - R_1 \cdot (0.25) - R_2 \cdot (0.75) = 0$$

$$F = 0.5R_1 + 1.5R_2$$

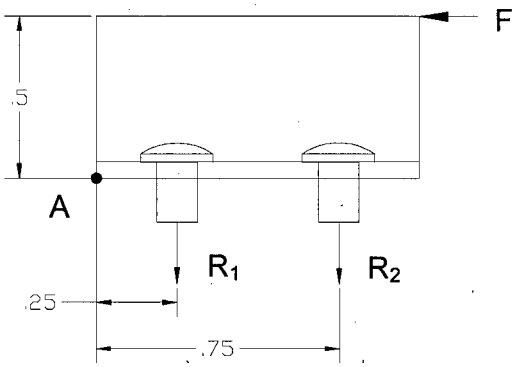

Figure 2.5-5 – Screw Prying Diagram

The relation between the screws is:

$$\frac{R_1}{R_2} = \frac{0.25}{0.75}$$

$$R_1 = \frac{1}{3} R_2$$

Substitute into the sum of moments equation:

$$F = 0.5R_1 + 1.5R_2$$

$$F = (\frac{1}{3} 0.5R_2) + 1.5R_2$$

$$R_2 = 0.6F \text{ lb}$$

$$R_1 = 0.2F \text{ lb}$$

The peak tension appears in R_2. The maximum tensile stress is:

$$\sigma = \frac{R_2}{A_s} = \frac{0.6F}{0.0152} = 39.47F \text{ psi}$$

Combine the shear and tensile stresses to find the force necessary to fail the screws:

$$\sigma_{ultimate} = \sqrt{\sigma^2 + 4\tau^2} = \sqrt{(39.47F)^2 + 4(35.46F)^2}$$

$$144{,}000 = \sqrt{6{,}588F^2} = 81.17F$$

$$F = 1{,}774 \text{ lb}$$

2.5.3.2 Locking Pin Loading

To show that the handle attachment fails prior to the closure components of the package, the force necessary to fail the screws is applied to the two locking pins. The yield strength of the locking pins is conservatively used in the comparison.

The locking pins are 0.25 inch in diameter and made of ASTM A276, Type S21800 material, having a yield strength of σ_{yield} = 50,000 psi. The pin area is:

$$A_p = \frac{\pi d^2}{4} = \frac{\pi(.25)^2}{4} = 0.049 \text{in}^2$$

The load *P* must be calculated from the screw failure load *F*. The distance from the center of the closure assembly to the point of shear in the locking pin is half of the diameter of the closure at the location of the pin, or r_p = 5.97/2 = 2.99 inches. The distance from the center of the closure assembly to the load *F* is 3.25 inches.

$$P = \frac{3.25F}{2.99} = 1{,}928 \text{ lb}$$

The shear stress for each pin is:

$$\tau = \frac{1}{2} \cdot \frac{P}{A} = \frac{1{,}928}{2(.049)} = 19{,}673 \text{ psi}$$

The margin of safety on the locking pins (against pin yield) at the point of handle screw failure is:

$$MS = \frac{0.6\sigma_{yield}}{\tau} - 1 = \frac{0.6 \times 50{,}000}{19{,}673} - 1 = +0.52$$

where the factor of 0.6 converts the tensile yield of the pin material to shear yield. Thus, should the closure handle be incorrectly used as a tiedown device, the handle screws will break off before the pins yield.

2.5.3.3 Conclusion

From the above analysis, should a force be applied to the closure handle, the handle screws will fail before the closure locking pins yield. Therefore, adverse loading of the closure handle does not impair the ability of the package to meet other requirements.

2.6 Normal Conditions of Transport

2.6.1 Heat

2.6.1.1 Summary of Pressures and Temperatures

As presented in Table 3.1-1 of Section 3.1.3, *Summary Tables of Temperatures*, the maximum ATR FFSC package temperature under conditions of 100°F ambient temperature and full insolation is 186°F on the outer shell. As presented in Table 3.1-2 of Section 3.1.4, *Summary Table of Maximum Pressures*, the maximum normal operating pressure (MNOP) of the ATR FFSC package is zero. This is assured because there are no seals provided between the body and closure to retain pressure.

The ATR FFSC body cavity is also discussed in Section 3.1.4, *Summary Table of Maximum Pressures*. The maximum pressure that may develop between the inner and outer shells will be limited to that achieved due to ideal gas expansion. The maximum pressure rise within the sealed cavity under NCT will be less than 4 psi gauge.

2.6.1.2 Differential Thermal Expansion

Because of the simple design of the ATR FFSC package, there are no features, such as rigid lids and containment seals, which could be affected by the differential thermal expansion of the package components. In addition, since the package has a negligible internal decay heat, any temperature differences will arise only from the solar loading, and consequently be modest in nature.

The nominal end gap between the package cavity and the FHEs (ATR, MIT, MURR, and RINSC) or the LFPB is 0.63 inches and 0.38 inches respectively. These gaps are large enough to prevent the payload from expanding enough to load the closure. Therefore, differential thermal expansion is not of concern.

2.6.1.3 Stress Calculations

Since the MNOP is zero and the maximum sealed cavity pressure is 4 psi gauge, stresses due to NCT pressures and temperatures are negligible.

2.6.1.4 Comparison with Allowable Stresses

Since NCT stresses are negligible, this section does not apply.

2.6.2 Cold

With an internal decay heat load of zero, no insolation, and an ambient temperature of -40°F, the average package temperature will be -40°F. None of the materials of construction (i.e., stainless steel) undergo a ductile-to-brittle transition at temperatures of -40 °F or higher. Therefore, the minimum NCT temperature is of negligible consequence.

2.6.3 Reduced External Pressure

As discussed in Section 2.6.1.1, *Summary of Pressures and Temperatures*, the ATR FFSC packaging is not capable of retaining pressure. Therefore, there is no effect of a reduced external pressure on the package of 3.5 lbf/in^2 (25 kPa) absolute, per 10 CFR §71.71(c)(3).

2.6.4 Increased External Pressure

10 CFR §71.71(c)(4) requires exposure of the ATR FFSC package to an increased external pressure of 20 psi (140 kPa) absolute. Since there are no sealing surfaces, there is no effect of an increased external pressure to the ATR FFSC package.

Section 2.7.6.1, *Cavity Evaluation*, evaluates the effect of pressure on the sealed cavity between the outer 8 inch tube and inner 6 inch diameter pipe. This cavity is welded closed during fabrication and has no relation to the payload. The cavity evaluation conservatively considers the satisfactory performance of a 22 psi gauge external pressure to the packaging.

2.6.5 Vibration

The effects of vibration normally incident to transport are not significant for the ATR FFSC packaging. Table 2 of ANSI N14.23[7] shows peak vibration accelerations of a trailer bed as a function of package and tie-down system natural frequency. For the frequency range 0 to 5 Hz, assuming a light package, Table 2 of ANSI N14.23 gives peak accelerations (99% level) of 2g in the vertical direction, and 0.1g in both the lateral and longitudinal directions. All other frequency ranges give significantly lower acceleration levels.

The ATR FFSC is very resistant to damage from transportation vibration. The closure is subject to the ± 0.1g longitudinal (axial) loading, but since friction between the closure and its opening will exceed 0.1, the closure is not expected to apply any vibrational loadings to the bayonet lugs. The insulating material located between the inner, round tube and the outer, square tube is retained in place by a jacket of 28 gauge stainless steel. The resistance to displacement of the insulation was demonstrated in the testing program (see Section 2.12.2.5.1, *CTU Inspection*). When exposed to axial impacts which were many times larger than the vibration load of 0.1g, the insulation displaced an insignificant distance which was bounded by the assumptions made in the thermal analysis. Therefore, vibration will have no effect on the placement or condition of the insulation.

When supported on the shipping rack, the package is supported near index lugs which interface with the two pockets on the lower face of the package. Conservatively, an analysis of the package as a simply supported beam, supported at the extreme ends, is performed. The overall length of the package is L = 72.5 inches, and the maximum weight, from Table 2.1-1, is 290 lb. The distributed load is therefore 290/72.5 = 4 lb/in. The outer square tube has a square

[7] ANSI N14.23, *Design Basis for Resistance to Shock and Vibration of Radioactive Material Packages Greater Than One Ton in Truck Transport*, 1980, American National Standards Institute, Inc. (ANSI).

dimension of 8 inches and a wall thickness of 0.188 inches. AISC[8] gives the moment of inertia of the tube as 58.2 in^4. The c-distance is 4 inches. The bending moment is:

$$M = \frac{wL^2}{8}(2) = 5{,}256\ in \cdot lb$$

where the factor of 2 accounts for the inertia loading of ± 2g. The reversing bending stress in the outer square tube is:

$$\sigma = \frac{Mc}{I} = 361\ \text{psi}$$

This value is well below the fatigue limit for stainless steel. Since the inner round tube is supported at three places along its length, the unsupported length is much shorter than for the outer square tube. In addition, the distributed weight, which consists of only the self-weight and payload weight, is significantly less than for the outer square tube. For these reasons, the stress in the inner round tube will be bounded by the stress in the outer square tube.

The FHEs and loose fuel plate basket are designed to be form fitting and supported by the inner stainless steel round tube. Furthermore, the FHEs and loose fuel plate basket are completely removed and in view at both the shipping and receiving sites, and consequently, a complete fatigue failure of either basket due to transportation vibration is not to be expected.

For these reasons, the effect of vibration normally incident to transport is not of concern for the ATR FFSC package.

2.6.6 Water Spray

The external surfaces of the ATR FFSC package are made from stainless steel, whose properties are not affected by water spray. For this reason, the effect of water spray, per 10 CFR §71.71(c)(6), is not of concern for the ATR FFSC package.

2.6.7 Free Drop

10 CFR §71.71(c)(7) requires a free drop for the ATR FFSC package. Since the package gross weight is less than 11,000 lb, the applicable free drop distance is 4 ft. As discussed in Appendix 2.12.1, *Certification Tests on CTU-1,* one NCT free drop preceded the HAC drop tests performed on CTU-1. The damage from the NTC drop case was minor as illustrated in Figure 2.12.1-5 through Figure 2.12.1-7. There was no loss or dispersal of package contents, and no substantial reduction in the effectiveness of the packaging. The latter result was confirmed by the successful completion of the subsequent HAC testing.

From the test results, the amount of deformation in the top corner was approximately 1/8 inch. Because there are no crushable materials of construction, the deformation of the package in any other NCT drop orientation is assumed to be the same or less than this CG over top corner

[8] American Institute of Steel Construction, *Manual of Steel Construction, Allowable Stress Design*, Ninth Edition, 1989.

orientation. This assumption is verified by the degree of damage recorded during the HAC drop orientations discussed in Section 2.7, *Hypothetical Accident Conditions.*

By observation, the NCT damage is much less than 5% of the total effective volume of the package, approximately 230 in^3, based on 5% of the volume of the 72.5-inch long, by 8-inch square tube. Therefore, the requirement of 10 CFR §71.55(d)(4)(i) is met. Further, the effective spacing between fissile contents is 8 inches, based on a center-to-center distance between packages which are in side to side and top to bottom contact. Five percent of this distance is 0.4 inches, and therefore the requirement of 10 CFR §71.55(d)(4)(ii) is met. Finally, no opening capable of admitting a 4-inch cube was created, and the requirement of 10 CFR §71.55(d)(4)(iii) is also met. Thus, the effect of the free drop test, per 10 CFR §71.71(c)(7), is not of concern.

2.6.8 Corner Drop

This test does not apply, since the ATR FFSC package is a rectangular fissile material package weighing more than 110 lb, as specified in 10 CFR §71.71(c)(8).

2.6.9 Compression

As specified in 10 CFR §71.71(c)(9), the ATR FFSC must be subjected, for a period of 24 hours, to a compressive load applied uniformly to the top and bottom of the package in the normal transport position. The greater of the following uniformly distributed loads is to be used: (a) the equivalent of 5 times the weight of the package, or (b) the equivalent of 2 lbf/in^2 multiplied by the vertically projected area of the package. For these two cases, the loads are:

$$P_{(a)} = 5 \cdot W = 5 \cdot 290 lbf = 1{,}450\ lbf$$

$$P_{(b)} = 2\ psi \cdot L \cdot w = 2\ psi \cdot (72.5\ in) \cdot (8\ in) = 1{,}160\ lbf$$

Where,

W is the maximum weight of one package

w is the overall width of the package

L is the overall length of the package.

Thus, it is seen that case (a) governs with a compressive load of 1,450 lbf.

The exterior side of the ATR FFSC packaging is a reinforced 8 inch by 8 inch square stainless steel tube with a 0.188 inch wall thickness. The closure end includes a 1.5 inch thick stainless steel plate and the bottom end includes a 0.88 inch thick stainless steel plate. By observation, buckling of the outer tube is not a concern due to its reinforcement, short height, wall thickness, and the relatively small load applied. A conservative evaluation is performed in the following section to demonstrate the adequacy of the design under the compression load.

2.6.9.1 Compression Evaluation

To conservatively evaluate the compressive load, buckling of the square tube under a uniform load is evaluated neglecting the reinforcing end plates and interior ribs. The applied load, as determined in Section 2.6.9, *Compression*, is 1,450 lbf. The average stress in the 8 inch tube is:

$$\sigma_{tube} = \frac{P}{A_{tube}}$$

Where,

P = applied load = 1,450 lbf

A_{tube} = area of vertical legs of the tube = 2 x t x L $= 2 \cdot (0.19) \cdot 72.5 = 27.6 in^2$

t = thickness = 0.19 in

L = length of tube = 72.5 in

Therefore:

$$\sigma_{tube} = \frac{P}{A_{tube}} = \frac{1450}{27.6} = 52.5\ psi$$

Using Roark[9], Table 35 Case 1a, a rectangular plate under equal uniform compression, all edges simply supported, the critical unit compressive stress σ' is:

$$\sigma' = K \cdot \frac{E}{1 - v^2} \cdot \left(\frac{t}{L}\right)^2$$

Where,

E = modulus of elasticity for stainless steel = 27.6 Mpsi

v = Poisson's ratio = 0.3

K = conservatively chosen as equal to 10.9

$$\sigma' = 10.9 \cdot \frac{27600000}{1 - (.3)^2} \cdot \left(\frac{0.19}{72.5}\right)^2 = 2{,}271\ psi$$

By comparison:

$$\sigma_{tube} << \sigma'$$

Therefore, buckling of the outer tube due to the compression load is not a concern.

2.6.10 Penetration

10 CFR §71.71(c)(10) requires that a bar of hemispherical end, weighing at least 13 lb be dropped from a height of 40 inches onto the most vulnerable part of the packaging. As

[9] Young, Warren C., *Roark's Formulas for Stress and Strain*, Sixth Edition, 1989, McGraw Hill, New York, New York.

documented in Appendix 2.12.1, *Certification Tests on CTU-1*, the ATR FFSC package, weighing approximately 290 lb, was subjected to the much more demanding test of being dropped from 40 inches onto the puncture bar described in §71.73(c)(3) without experiencing any damage which could compromise confinement or criticality control. Therefore, this test does not need to be performed, and the penetration test requirement is satisfied.

2.7 Hypothetical Accident Conditions

When subjected to the hypothetical accident conditions of 10 CFR §71.73, the ATR FFSC prevents loss or dispersal of the enriched uranium payload. The analysis given in Chapter 6, *Criticality*, which includes conservative assumptions regarding damaged geometry and moderation, demonstrates the criticality safety of the ATR FFSC under hypothetical accident conditions.

10 CFR §71.55 requires that packages containing fissile material be evaluated for criticality with the inclusion of any damage resulting from the NCT tests specified in §71.71 plus the damage from the HAC tests specified in §71.73. The ATR FFSC was subjected to accident condition loadings by means of full scale certification testing. Each test specified by §71.73 was applied sequentially, as specified in Regulatory Guide 7.8[10]. One full scale certification test unit (CTU-1) using the ATR fuel element as the payload was subjected to the full series of free drop and puncture testing. A second full scale certification test unit (CTU-2) using the loose fuel plates as the payload was subjected to a series of worst case free drops. Puncture drops were not performed on CTU-2 because the testing focused on the performance of the insulation and payload, which would not be affected by any puncture damage. The puncture testing performed on CTU-1 demonstrated that the effects of the puncture test on the insulation and on the payload are negligible. Utilizing the results of drop testing, the fire test was evaluated analytically. The immersion tests are also evaluated analytically.

The payload for CTU-1 used during testing was an un-irradiated ATR fuel element, enriched to a maximum of 94% U-235. The ATR fuel element used was a rejected production fuel element. The defects were considered cosmetic only and had no structural significance for purposes of the certification tests. Further discussion of the CTU-1 payload is provided in Appendix 2.12.1, *Certification Tests on CTU-1*.

The simulated loose fuel plate payload for CTU-2 was a combination of 2- and 4-inch wide, 0.06-inch thick, 5052H32 aluminum flat plates. All plates were 49.5 inches long. There were 15, 2-inch wide plates and 10, 4-inch wide plates. The weight of the aluminum plates totaled 20.7 lb. Further discussion of the CTU-2 payload is provided in Appendix 2.12.2, *Certification Tests on CTU-2*.

Rationale for the selection of the test series is given below. The tests actually performed, and their sequence, are summarized in Table 2.7-1. Test results are summarized in the sections which follow and in Section 2.7.8, *Summary of Damage*, with details given in Appendix 2.12.1, *Certification Tests on CTU-1* and Appendix 2.12.2, *Certification Tests on CTU-2*.

[10] U. S. Nuclear Regulatory Commission, Regulatory Guide 7.8, *Load Combinations for the Structural Analysis of Shipping Casks for Radioactive Material*, Revision 1, March 1989.

The performance of the MIT and MURR fuel elements is bounded by the test results using the ATR fuel element. A full discussion and comparison of the three fuel elements is given in Appendix 2.12.3, *Structural Evaluation for MIT and MURR Fuel.* As with the ATR fuel element, the criticality evaluation performed in Section 6.10, *Appendix B: Criticality Analysis for MIT and MURR Fuel*, makes conservative assumptions designed to encompass a wide range of damage exceeding the actual damage observed during testing of the ATR fuel element. Since Section 6.11, *Appendix C: Criticality Analysis for RINSC Fuel* conservatively models the fuel as a homogeneous mixture of uranium and water, a structural evaluation of the RINSC fuel element and the corresponding FHE is not required.

2.7.1 Free Drop

10 CFR §71.73(c)(1) requires a free drop of the specimen through a distance of 30 ft onto a flat, essentially unyielding surface in the orientation for which maximum damage is expected. The primary mode of failure of the ATR FFSC would be loss of the ability of the closure to retain the payload. This could occur through loss of the bayonet style lugs, or through failure of the retracting pins allowing the lid to rotate, or through excessive deformation of the closure area which could cause separation of the body from the closure. If a sufficient gap is formed between the body and closure, the payload may no longer be retained, consequently possibly affecting criticality safety.

The object of the free drop tests in the current instance is to create the maximum amount of damage in critical locations and components. Therefore, free drop orientations are selected which would result in the greatest amount of critical damage and which would render the package most vulnerable to damage from the puncture drop test.

The ability of the payload to remain in a critically safe geometry is also confirmed through the free drop tests. Following all drop tests, the fuel assembly in CTU-1 and the simulated loose fuel plates in CTU-2, are inspected to confirm the geometries remain within the assumptions used in Section 6.0, *Criticality Evaluation.*

To confirm the performance of the payload at reduced temperatures CTU-1 was subjected to two HAC drops with the payload temperature at approximately -20°F (-29°C). Following all CTU-1 testing, as discussed in Appendix 2.12.1, *Certification Tests on CTU-1*, the package was destructively disassembled and the payload inspected.

Upon inspection of both CTU-1 and CTU-2, the performance of both the payload and packaging, including the reduced temperature tests, was satisfactory.

2.7.1.1 Side Drop

The horizontal side drops for CTU-1 include CD1-1, CD2-1, and CD3-1. The first three HAC drops primarily address the packaging closure and shell response to the free drops. Also, the side drop orientations represent large impact loads to the ATR fuel element for geometry control. CD1-1 presents the highest acceleration to the locking pins when the pins are oriented vertically with respect to the target surface. CD2-1 is directed at challenging the outer shell in the vicinity of the index lugs. The intent is to demonstrate that the outer shell is not penetrated by the impacted index lugs which could represent a thermal concern. In CD3-1, the locking pins are oriented horizontally with respect to the target surface presenting the worst case bending load to the locking feature.

The horizontal side drops for CTU-2 include CD1-2 and CD3-2. These two HAC drops address the performance of the LFPB in maintaining the geometry of the loose plates. Furthermore, the intent is to demonstrate the similar performance of the outer packaging in response to the LFPB as the payload.

2.7.1.2 CG Over Bottom Drop

The CG over bottom drop for CTU-1 includes CD4-1. This vertical orientation is expected to have the greatest potential for deformation to the insulation cavity at the bottom end. CD4-1 is considered to present the worst case loading to the 3/8 inch thick plate located at the bottom of the payload cavity. The intent of the drop is to demonstrate the insulation cavity at the bottom end of the package is not breached or significantly reduced. Additionally, the CD4-1 drop presents the worst case buckling load to the ATR fuel element.

For CTU-2, the CG over bottom drop includes CD4-2. As with CD4-1, this orientation is expected to have the greatest local deformation to the bottom end plate and insulation cavity and present the worst case buckling load to the LFPB and loose plates.

2.7.1.3 CG Over Corner Drop

The CG over corner drop was only performed on CTU-1. CD5-1, the CG over top corner drop, produces the greatest deformation in the closure region and also presents the greatest challenge for the closure locking tabs. The intent of the drop is to demonstrate the effectiveness of the closure in retaining the payload.

2.7.1.4 Oblique Drops

An oblique free drop orientation, also known as a slap-down drop, was not performed for this package. Consequences from the slap-down event are considered bounded by the CG over bottom (CD4-1/CD4-2) and CG over corner (CD5-1) drop tests performed. The slap-down drop challenges the closure and the fuel by producing high angular velocities and accelerations to the packaging and contents. However, in the case of the ATR FFSC, the end drops present a greater challenge to the closure and the fuel than the slap-down condition. In bolted closure designs, the slap-down side loads have the tendency to shear the closure bolts. Since the ATR FFSC closure is secured by a bayonet type design rather than bolts, this is not a concern. The axial load imparted to the closure in a slap-down drop will be lower than the axial loading developed in an end drop. And the greater the axial load, the greater the challenge to the locking tabs on the closure. The CD5-1 drop therefore presents the greatest challenge to closure retention, and the CD4-1/CD4-2 drop presents the greatest potential for fuel buckling.

2.7.1.5 Results of the Free Drop Tests

CD1-1 Flat Side Drop (CTU-1). See Figure 2.12.1-8 through Figure 2.12.1-13. The visible damage resulting from the 30 ft flat side drop, pocket side down, was negligible. There were minor visible exterior scratches resulting from the drop. The areas showing the greatest impact marks are at each end plate and near the three internal stiffening ribs. There was no significant bowing or other visible deformation. There was no visible deformation or rotation of the closure and the locking pins remained in the locked position.

Following the CD1-1 drop, CTU-1 was opened and the FHE and fuel element payload were visually inspected for damage. As illustrated in Figure 2.12.1-11 in Section 2.12.1, there were no major deformations and no cracked welds noticed. As illustrated in Figure 2.12.1-12, there was no visible damage to the fuel element.

With the closure assembly removed from the body of the CTU, one locking pin was noticeably bent approximately 1/32 inch as illustrated in Figure 2.12.1-13. It was noticed that the bent locking pin tended to bind when compressed to the open position. The other locking pin was not deformed and there was no other visible deformation of the closure assembly.

CD2-1 Flat Side Drop (CTU-1). Due to CTU-1 not impacting square on the index lugs, this orientation was tested three different times. The three tests in this orientation are identified as CD2.A-1, CD2.B-1, and CD2.C-1 throughout this section. For CD2.A-1, CTU-1 rotated during its descent and impacted at a slight angle causing the package to bounce and spin somewhat on the longitudinal axis after impact. The visible damage resulting from the CD2.A-1 drop was minor with the index lugs at each end pressed into the body approximately 1/8 inch. See Figure 2.12.1-14 through Figure 2.12.1-17.

For CD2.B-1 the package again rotated during its decent and impacted at an angle causing the package to bounce and spin on the longitudinal axis after impact. Also, a gust of wind blew the rigging straps into the adjacent stadia board during the drop. The visible damage resulting from the CD2.B-1 drop was minor with the index lugs at each end now pressed into the body approximately 3/16 inch. See Figure 2.12.1-18 through Figure 2.12.1-20.

CD2.C-1, which was performed after CD5-1, impacted in the correct orientation directly on the index lugs; see Figure 2.12.1-37 through Figure 2.12.1-40. The index lug near the closure end was flush with the original surface, pressed in approximately 3/8 inch (the height of the lug) as seen in Figure 2.12.1-39. The index lug at the bottom end was pushed in to approximately 1/8 inch from the original surface. A cracked weld was found under the index lug near the closure end as shown in Figure 2.12.1-40. The length of the cracked weld was approximately ½ inch.

CD3-1 Flat Side Drop – Reduced Temperature (CTU-1). See Figure 2.12.1-22 through Figure 2.12.1-25. The visible damage resulting from the 30 ft flat side drop performed with the payload at reduced temperature (-20°F) was negligible. Similar to CD1-1, the impact side exhibited scratches and impact marks near the locations of the internal ribs. Upon inspection of the closure assembly, one of the two locking pins was found sheared off from the outside edge of the closure as it interfaces with the package body. There was no other visible damage or any signs of rotation to the closure assembly as the second locking pin remained in the locked position.

CD4-1 CG Over Bottom End – Reduced Temperature (CTU-1). See Figure 2.12.1-26 through Figure 2.12.1-28. The visible damage resulting from the 30 ft CG over bottom end drop performed with the payload at reduced temperature (-20°F) was minor. The outer shell of CTU-1 exhibited minor bowing near the impact end with the greatest deformation measuring approximately 1/8 inch on one side. The overall length of the package body was compared with the initial measurements at eight locations and found to have compressed a maximum of approximately 1/8 inch. There was no visible deformation or rotation of the closure following the drop and the remaining locking pin remained in the locked position.

CD5-1 CG Over Top Corner Drop (CTU-1). See Figure 2.12.1-32 through Figure 2.12.1-36. The visible damage resulting from the 30 ft CG over top corner drop was prominent in the

closure area. The impact corner was deformed in approximately 5/8 inch. There was modest deformation on the sides of the package near the impact location bulging in approximately 1/2 inch near the index lug pocket and bulged out approximately 5/8 inches on the adjoining side.

Following the drop, the closure assembly exhibited deformation with the end of the package and was unable to be rotated more than 1/8 inch in either direction. The locking pins showed no visible signs of deformation and the remaining locking pin remained in the locked position.

CD1-2 Flat Side Drop (CTU-2). See Figure 2.12.2-5 through Figure 2.12.2-7. This drop is a repeat of CD1-1 using the loose fuel plate payload rather than the ATR fuel element. The orientation of the LFPB parting lines is shown in Figure 2.12.2-3 through Figure 2.12.2-4. There was minor visible exterior damage, principally scuff marks, resulting from the drop. There was no bowing or other significant visible deformation. There was no visible deformation or rotation of the closure assembly, and the locking pins were unaffected by the drop.

Following the CD1-2 drop, CTU-2 was opened and the LFPB and payload were inspected. The basket was not affected by the drop, however the finger operated screws securing the two basket halves were loosened slightly. One tie wrap was broken but the simulated loose fuel plates were not damaged. The broken tie wrap was not replaced for the subsequent drops.

CD3-2 Flat Side Drop (CTU-2). See Figure 2.12.2-8 through Figure 2.12.2-10. This drop is a repeat of CD3-1 but at ambient temperature and using the loose fuel plate payload rather than the ATR fuel element. As with the other side drop events, the outer shell exhibited minor impact marks at the stiffening rib locations. There was no visible deformation or rotation of the closure assembly, and the locking pins were undamaged and in good working order.

The closure was opened and the payload inspected following the CD3-2 drop. The basket exhibited no signs of deformation and again the basket screws were loosened slightly. The second plastic tie wrap was broken and the simulated fuel plates exhibited no significant damage as seen in Figure 2.12.2-10. The broken tie wrap was not replaced for the subsequent drop.

CD4-2 CG Over Bottom End (CTU-2). See Figure 2.12.2-11 through Figure 2.12.2-16. This drop orientation is a repeat of CD4-1 but at ambient temperature and using the loose fuel plate payload rather than the ATR fuel element. CTU-2 appeared to impact slightly off of true vertical and impacted near one corner of the package. The impact caused one side to dent inward approximately ½ inch and the adjacent side to bulge out approximately ½ inch. There was no overall bowing of the package or other significant visible deformation. There was no visible damage to the closure or the locking pins.

The closure was removed and the basket extracted following the CD4-2 drop. The basket damage was minor and limited to a small dent at the end of the basket that was situated closest to the package bottom and a small deformation to the basket end plate from the package inner shell. As illustrated in Figure 2.12.2-15 and Figure 2.12.2-16, the simulated fuel plates experienced localized deformation at the end of the basket closest to the package bottom. The remaining area above the localized deformation was not deformed.

The gap between the thermal shield and the stiffening rib, where the shield pulls away from the rib was found to be less than 1/16-inch during the disassembly of CTU-2 discussed in Section 2.7.8.2, *CTU-2 Package Disassembly – Results*. With the thermal shields removed the maximum compaction for all insulation sections ranged from 1 inch to 1¾ inches.

2.7.2 Crush

10 CFR §71.73(c)(2) requires that the crush test be performed on fissile material packages which have a mass not greater than 1,100 lb and a density not greater than 62.4 lb/ft^3. The ATR FFSC package has a maximum weight of 290 lb and a volume of 2.69 ft^3 (based on outside dimensions of 8 in x 8 in x 72.5 in), leading to a maximum density of 290/2.69 = 108 lb/ft^3. Therefore, the crush test is not applicable.

2.7.3 Puncture

10 CFR §71.73(c)(3) requires the drop of the package onto a 6-inch diameter steel bar from a height of 40 inches. The primary modes of failure of the ATR FFSC would be closure damage, closure rotation, and penetration of the outer shell. The object of the puncture drop tests in the current instance is to create the maximum amount of damage in critical locations and components. Therefore, drop orientations are selected which would result in the greatest amount of critical damage and which would render the package most vulnerable to the thermal event. For the ATR FFSC, these are the CG over center of closure, 30° oblique CG over side, and an oblique drop onto the closure.

The CG over center of closure position was chosen to confirm the performance of the closure assembly and verify at least one locking pin remained locked to prevent rotation. The 30° oblique CG over side was chosen to confirm the resistance of the outer shell to penetration from the puncture bar. The oblique drop onto the closure assembly confirms that the puncture bar can not cause rotation of the closure and was added after the CD3-1 drop sheared one of the locking pins.

CTU-2 was not subjected to puncture, since the purpose of the CTU-2 test unit was to demonstrate the effectiveness of the LFPB and the performance of the thermal insulation. The puncture test would have no impact on these features.

2.7.3.1 Results of the Puncture Tests

CG Over Center of Closure, Vertical (CP1-1). See Figure 2.12.1-44 through Figure 2.12.1-46. The puncture bar impacted directly on the closure assembly (the handle was removed during previous free drop tests). The drop resulted in only minor damage with the TID post deformed into the closure and the closure assembly exhibiting minor scratches from the puncture bar. The locking pins showed no visible signs of deformation and the remaining functional locking pin remained in the locked position.

CG Over Side, 30° Oblique (CP2-1). See Figure 2.12.1-41 through Figure 2.12.1-43. The initial impact caused a deformation of approximately 1/2 inch deep by 5 inches across with a radius the same as the puncture bar. There were no tears or fissures in the ATR FFSC outer skin and there was no change to the closure assembly.

Oblique Drop onto Closure (CP3-1). See Figure 2.12.1-29 through Figure 2.12.1-31. CP3-1 was an unscheduled puncture drop with the purpose of causing rotation to the closure assembly. This extra drop was chosen due to the failure of one of two locking pins during CD3-1. The puncture bar squarely impacted the closure rib and the CTU bounced away from the puncture bar onto the drop pad. Following the drop, the closure assembly rib exhibited minor deformations at the

impact point made by the puncture bar. There was no rotation of the closure, and the remaining functional locking pin remained in the locked position and showed no visible signs of deformation.

2.7.4 Thermal

10 CFR §71.73(c)(4) requires the exposure of the ATR FFSC packaging to a hypothetical fire event. Performance of the package under the thermal event is addressed analytically in Chapter 3, *Thermal Evaluation.* Disassembly of the package following the structural tests confirmed that the compaction to the insulation features, as assumed in the thermal analyses, was shown to still perform in a satisfactory manner.

2.7.4.1 Summary of Pressures and Temperatures

As shown in Section 3.4.3, *Maximum Temperatures and Pressures*, the maximum peak temperature of the outer shell was evaluated to be 1,471°F. The annular space between the outer shell and inner shell pressurized to a maximum 39 psi gauge during the HAC thermal event. The payload cavity of the ATR FFSC is vented to the atmosphere and therefore the inner shell (6 inch diameter pipe) experiences an external pressure of 39 psi gauge. Since the ATR FFSC does not provide leaktight containment, this pressure is not significant to the package.

2.7.4.2 Differential Thermal Expansion

The thermal analysis presented in Section 3.4.4, *Thermal Evaluation under Hypothetical Accident Conditions,* identifies that the peak temperature difference between the inner and outer shells occurs approximately six minutes into the thermal event and results in a free differential thermal expansion of approximately 0.9-inches between the two shells. This places the outer shell in compression and the inner shell in tension. The packaging could respond structurally to the forces developed by this differential expansion by:

- failure of one of the two inner shell to end plate welds (allowing free expansion of the outer shell relative to the inner shell), or
- no weld failure, but buckling of the outer shell, or
- a combination of the above two scenarios.

In any case, none of theses scenarios results in a geometry change to the packaging that leads to an increase in reactivity. The only concern is a condition that could allow an increase in heat transfer to the fuel such that the fuel approaches the melting point.

As identified in Section 3.4.4, *Thermal Evaluation under Hypothetical Accident Conditions,* the thermal consequences of the above events results in insignificant changes to the fuel temperature. The fuel does not approach the melting point and therefore there will be no impact to reactivity. The effect of differential thermal expansion on the various packaging components is therefore considered negligible.

At 72°F, the nominal length of the packaging cavity is 67.88 inches, the nominal length of the FHE is 67.25 inches and the nominal length of the LFPB is 67.5 inches. Both the LFPB and the FHE are fabricated from aluminum so the worst case for potential interference due to thermal expansion is with the LFPB. From Figure 3.4-5 it can be seen that above 700°F the inner shell

temperature is much greater than the LFPB temperature and so the inner shell thermal expansion rate exceeds that of the LFPB. During the cooling period below 700°F, the temperatures of the two components track within about 50 °F with the inner shell temperature always less than the LFPB. The worst condition for potential thermal expansion interference is near the peak temperature of the LFPB. For this evaluation, conservatively assume the LFPB temperature is 750°F and the inner shell is at 700°F. The length of the two components at these temperatures is calculated as follows:

$$L = \alpha \cdot L_{Original} \cdot (\Delta T) + L_{Original}$$

Where,

$L_{Original}$ = the original length of the component at 72°F

α = the coefficient of thermal expansion[11]

For aluminum: $\alpha_{Al} = 14.7(10^{-6})$ in/in/° F at 750 °F

For stainless steel: $\alpha_{SST} = 10.0(10^{-6})$ in/in/° F at 700 °F

ΔT = the change in temperature from 72°F

L = the length of the component at the elevated temperature

Loose fuel plate basket length at 750°F is:

$$L_{LFPB} = 14.7(10^{-6})(67.5)(750 - 72) + 67.5 = 68.17 \text{ inches}$$

Inner shell length at 700°F is:

$$L_{IS} = 10.0(10^{-6})(67.88)(700 - 72) + 67.88 = 68.31 \text{ inches}$$

$L_{IS} > L_{LFPB}$, therefore there is no interference under worst case conditions.

2.7.4.3 Stress Calculations

Since there is no differential thermal expansion interference between FHE or LFPB and the packaging, and since the packaging internal pressure is zero, there are no stresses to report.

2.7.4.4 Comparison with Allowable Stresses

Since there are no stresses to report, this section does not apply.

2.7.5 Immersion – Fissile Material

10 CFR §71.73(c)(5) requires performance of the immersion test for packages containing fissile material. The criticality evaluation presented in Chapter 6.0, *Criticality Evaluation*, assumes optimum hydrogenous moderation of single ATR FFSC packages and arrays of packages. Since the criticality consequences of water in-leakage are accounted for, and leakage of the payload from the packaging did not occur, the immersion test of 10 CFR §71.73(c)(5) is not of concern.

[11] Coefficients of thermal expansion are taken from ASME B&PV Code, Section II, Part D, coefficient B. For aluminum, Table TE-2, and for stainless steel, Table TE-1, Group 3.

2.7.6 Immersion – All Packages

10 CFR §71.73(c)(6) requires performance of an immersion test on an undamaged specimen under a head of water of at least 50 ft or 21.7 psig. The package payload cavity does not provide a leak tight containment. Since the criticality consequences of water in-leakage are accounted for, and leakage of the payload from the packaging did not occur, the immersion test of 10 CFR §71.73(c)(6) is not of concern.

The ATR FFSC does contain a sealed annular space between the outer square tube and the inner pipe where the insulation is located. The possible consequence of a 21.7 psig pressure applied to the outside surface of the square tube and the inside surface of the 6 inch diameter tube are considered insignificant to both the packaging and the payload.

2.7.7 Deep Water Immersion Test

The ATR FFSC package is a Type A Fissile package; hence, this requirement does not apply.

2.7.8 Summary of Damage

The discussions of sections 2.7.1, *Free Drop*, through 2.7.7, *Deep Water Immersion Test*, demonstrate that the ATR FFSC package prevents loss or dispersal of the payload when subjected to all applicable hypothetical accident tests. In addition, the ATR fuel element and loose fuel plates retain a geometry consistent with the analysis presented in Section 6.0, *Criticality Evaluation*. The physical test series consisted of multiple 30 ft free drop and puncture drop tests conservatively applied to two CTUs. Following the drop tests, each CTU was destructively disassembled to inspect various aspects of the packaging. Table 2.7-1 presents the certification drop test series in the sequential order performed for both CTU-1 and CTU-2.

Table 2.7-1 – ATR FFSC Certification Drop Test Series

Test No.	Test Description	Purpose of Test
CN1-1 (CTU-1)	CG over top corner	Confirm: • Fuel element does not penetrate the closure insulation pocket. • Fuel retains geometry necessary to maintain sub-criticality. • Closure is retained on the body and has not rotated relative to the package body.
CD1-1 (CTU-1)	Flat side drop, pocket side down.	Confirm: • Closure is retained and has not rotated relative to the package body. • Fuel retains geometry necessary to maintain sub-criticality.
CD2.A-1 (CTU-1)	Flat side drop, index lugs down	Confirm: • Impact on index lugs does not cause a fracture in the outer shell. • Closure is retained and has not rotated relative to the package body.
CD2.B-1 (CTU-1)	Flat side drop, index lugs down	Same purpose as CD2.A-1. This test was repeated due to the impact during CD2.A-1 being slightly rotated on the longitudinal axis and not fully impacting the index lugs.
CD3-1 (CTU-1)	Flat side drop, pocket and index lugs on side (-20°F)	Confirm: • Closure is retained and does not rotate relative to the package body. • Fuel element performance at cold temperature. • Fuel retains geometry necessary to maintain sub-criticality.
CD4-1 (CTU-1)	CG over bottom end (-20°F)	Confirm: • Fuel element does not penetrate into the packaging bottom end insulation pocket. This is a thermal performance requirement. • Fuel element performance at cold temperature. • Fuel retains geometry necessary to maintain sub-criticality.
CP3-1 (CTU-1)	Oblique drop onto closure assembly	Confirm: • Closure is retained on the body and does not rotate relative to the package body. This was an unscheduled test to confirm the performance of the remaining locking pin after the failure of the other pin during CD3-1.

Table 2.7-1 – ATR FFSC Certification Drop Test Series (continued)

Test No.	Test Description	Purpose of Test
CD5-1 (CTU-1)	CG over top corner (same orientation as CN1)	Confirm: • Fuel element does not penetrate the closure insulation pocket. • Fuel retains geometry necessary to maintain sub-criticality. • Closure is retained and does not rotate relative to the package body.
CD2.C-1 (CTU-1)	Flat side drop, index lugs down	Same purpose as CD2.A-1. This test was repeated for a third time due to the impact during CD2.B-1 being slightly rotated on the longitudinal axis and not fully impacting the index lugs.
CP2-1 (CTU-1)	CG over side, 30° oblique	Confirm: • Resistance of outer shell to puncture bar penetration.
CP1-1 (CTU-1)	CG over center of closure (Vertical)	Confirm: • Closure is retained and does not rotate relative to the package body.
CD1-2 (CTU-2)	Flat side drop, pocket side down.	Confirm: • Closure is retained and has not rotated relative to the package body. • Simulated fuel plates and basket retain geometry necessary to maintain sub-criticality.
CD3-2 (CTU-2)	Flat side drop, pocket and index lugs on side	Confirm: • Closure is retained and does not rotate relative to the package body. • Simulated fuel plates and basket retain geometry necessary to maintain sub-criticality.
CD4-2 (CTU-2)	CG over bottom end	Confirm: • Simulated fuel plates or basket do not penetrate into the packaging bottom end insulation pocket. This is a thermal performance requirement. • The insulation is not excessively compacted along the axial length of the package at the inner tube. • Simulated fuel plates and basket retain geometry necessary to maintain sub-criticality.

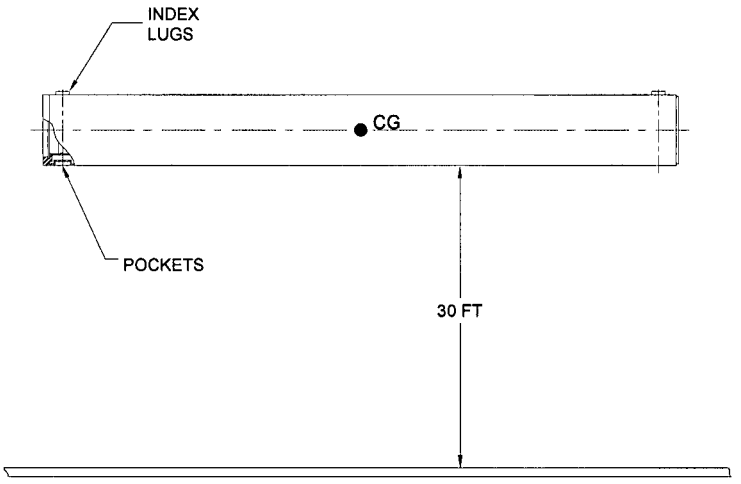

Index lugs and pockets rotated depending on drop series.

Figure 2.7-1 – ATR FFSC Certification Tests CD1-1, CD2-1, CD3-1, CD1-2, & CD3-2 (Test CD1-1 Shown)

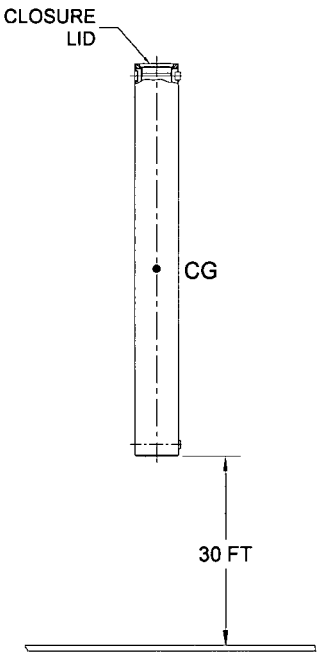

Figure 2.7-2– ATR FFSC Certification Tests CD4-1 & CD4-2

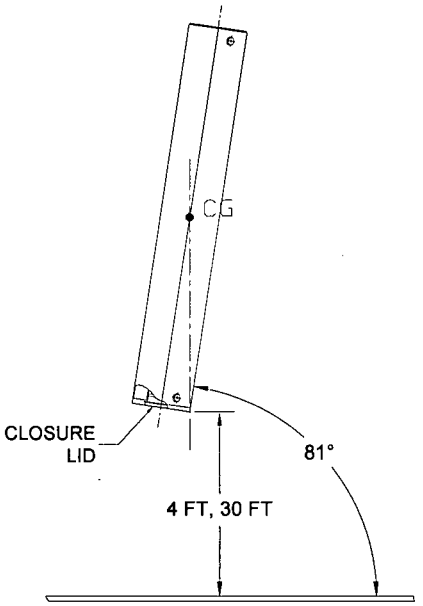

Figure 2.7-3 – ATR FFSC Certification Tests CN1-1 & CD5-1

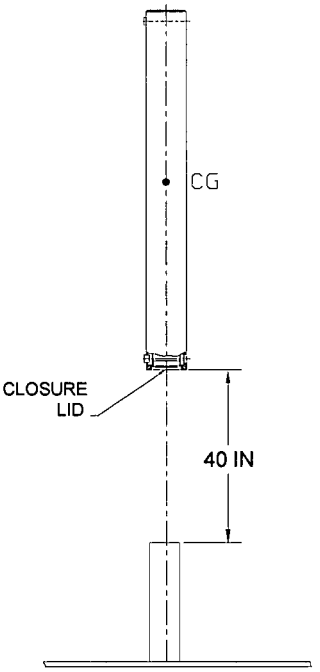

Figure 2.7-4– ATR FFSC Certification Test CP1-1

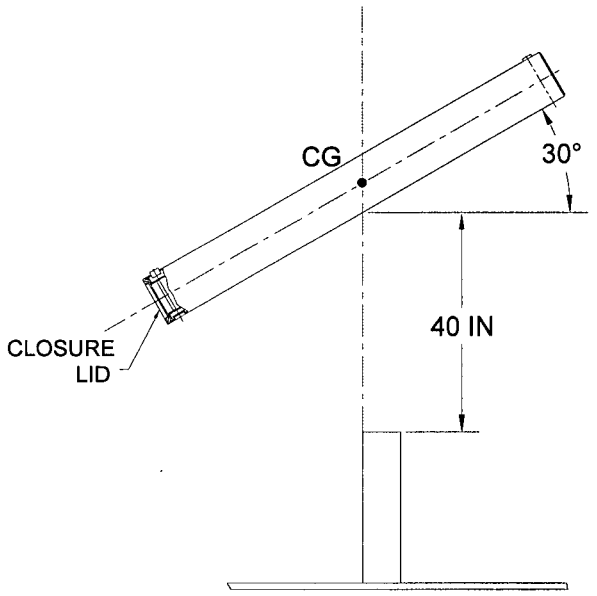

Figure 2.7-5– ATR FFSC Certification Test CP2-1

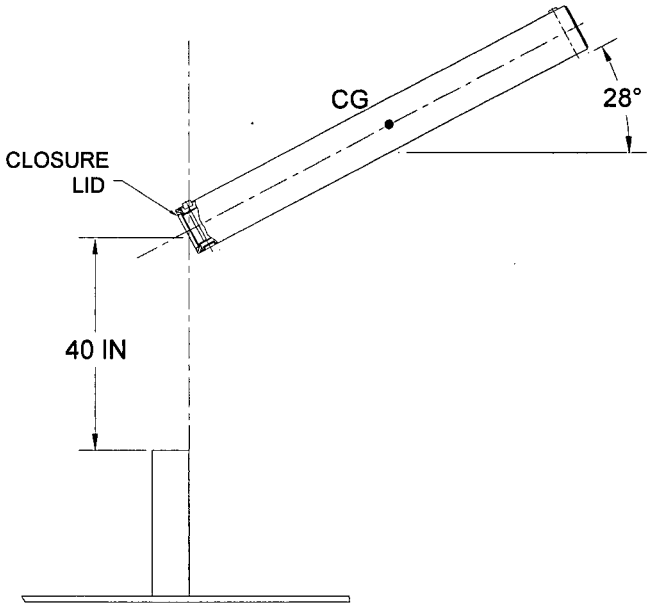

Figure 2.7-6– ATR FFSC Certification Test CP3-1

2.7.8.1 CTU-1 Package Disassembly - Results

Following the nine free drop tests and three punctures, CTU-1 was disassembled to examine the internal features. The items of critical importance focused on during the disassembly included:

- Loss or dispersal of any radioactive/fissile material
- Movement or compaction of the insulation material wrapped around the inner shell and condition of each end plate as related to the thermal evaluation.
- Deformations associated with the position and geometry of the ATR fuel element as related to the criticality evaluation.

To confirm the thermal performance features of the package the inner shell insulation and the insulation pockets at each end were visually inspected. The inner thermal shields remained in place and the maximum compaction for all insulation sections ranged from 1-1/8 inches to 1-½ inches. The closure end and bottom end insulation pockets were not penetrated and exhibited only minor deformation. For photographs of the disassembly see Figure 2.12.1-47 through Figure 2.12.1-51.

The inner tube was inspected as shown in Figure 2.12.1-52 and Figure 2.12.1-53. Due to the CG over corner drop deformation, CD5-1, the inner tube bowed out approximately ¼ inch in one localized area near the closure end. In the same area the inner tube also bowed inward approximately 3/16 inch slightly deforming the FHE aluminum end plate. There were no visible signs of any weld failures associated with the inner tube.

The FHE was removed from the inner shell and visually inspected as shown in Figure 2.12.1-56. The welds joining the endplates to the FHE body had failed at both ends. There was minor bowing and deformation located near the closure end of the package and some of the neoprene padding on the inside had become detached.

The ATR fuel element end boxes were shattered as expected. The geometry of the fissile material within the fuel element was not significantly altered and clearly was within the assumptions used in the criticality analysis as illustrated in Figure 2.12.1-57 through Figure 2.12.1-62. The post test inspection of the fuel element revealed large impact marks in the fuel plates as shown in Figure 2.12.1-58 through Figure 2.12.1-59 from fragments of the fuel element end boxes deforming the ends of the fuel plates. However, the uranium aluminide fissile material within each fuel plate was not exposed and the deformations at each end did not extend to the fissile material within each fuel plate. A comparison between the pre-test and post-test inspections of the fuel element is provided in Table 2.7-2. The measurements were generally taken at five locations along the length of the fuel plates. Note that, due to the numerous free drops and punctures applied to CTU-1, the damage experienced by the ATR fuel element was much greater than is to be expected for a single, 30 ft free drop and 40-inch puncture drop. Further detail is provided in Appendix 2.12.1, *Certification Tests on CTU-1.*

Table 2.7-2 – ATR Fuel Element Measurements

Measurement Area	Pre-Test Range (in)	Post-Test Range (in)
Side Plate Flatness	±0.010	±0.075
In-Plane Bending of Side Plates	±0.011	±0.025
Side Plate Spacing - Top	4.113 – 4.130	4.015 – 4.131
Side Plate Spacing - Bottom	1.840 – 1.845	1.837 – 1.845
Height of Top Fuel Plate from Table (top side up)	2.675 – 2.691	2.655 – 2.785
Height of Bottom Fuel Plate from Table (bottom side up)	2.500 – 2.540	2.415 – 2.508
Fuel Plate to Fuel Plate Spacing	0.075 to 0.080	0.023 to 0.098①

① The minimum and maximum fuel plate spacing measurements were in localized areas near the side vents and not representative of the general spacing.

2.7.8.2 CTU-2 Package Disassembly - Results

Following the three free drop tests, CTU-2 was disassembled to examine the internal features. The items of critical importance focused on during the disassembly included:

- Loss or dispersal of any parts of the simulated loose fuel plate payload.
- Movement or compaction of the insulation material wrapped around the inner shell and condition of each end plate as related to the thermal evaluation.
- Deformations associated with the position and geometry of the simulated loose fuel plates as related to the criticality evaluation.

To confirm the thermal performance features of the package the inner shell insulation and the insulation pockets at each end were visually inspected. The gap between the thermal shield and the stiffening rib, where the shield pulls away from the rib, is less than 1/16-inch. With the thermal shields removed the maximum compaction for all insulation sections ranged from 1 inch to 1 ¾ inches. The closure end and bottom end insulation pockets were not penetrated and exhibited only minor deformation. The bottom end plate was cut open and there was no indication of compression of the insulation in that region. For photographs of the disassembly see Figure 2.12.2-18 through Figure 2.12.2-27.

The inner tube was inspected and a minor deformation occurred near the bottom end of the package as shown in Figure 2.12.2-28 and Figure 2.12.2-29. The tube was bulged out approximately 1/16-inch and, closer to the end, an inward deformation of approximately ¼ inch.

These deformations were localized and did not impair free movement of the basket in the payload cavity. There were no visible signs of any weld failures associated with the inner tube.

Following each of the three drop tests the package was opened and both the LFPB and simulated fuel plates visually inspected. The damage to the LFPB was limited to a small dent at the end of the basket that was situated closest to the package bottom and the impact point as shown in Figure 2.12.2-14. The damage was minor and did not impair the ability of the LFPB to retain the simulated fuel plates.

The simulated fuel plates within the LFPB experienced visible deformation only during the CD4-2 drop. The plates experienced localized deformation at the end of the basket closest to the package bottom as seen in Figure 2.12.2-15 and Figure 2.12.2-16. Above this area the simulated fuel plates were not deformed. Further details can be found in Appendix 2.12.2, *Certification Tests on CTU-2.*

By meeting all of the structural approval standards of Subpart E of 10 CFR §71, the ATR FFSC ensures criticality safety of the package under normal conditions of transport and hypothetical accident conditions.

2.8 Accident Conditions for Air Transport of Plutonium

The ATR FFSC package does not transport plutonium; hence, this section does not apply.

2.9 Accident Conditions for Fissile Material Packages for Air Transport

The ATR FFSC package is not transported by air; hence, this section does not apply.

2.10 Special Form

The ATR FFSC payload is not in special form; hence, this section does not apply.

2.11 Fuel Rods

The ATR FFSC package does not carry irradiated fuel rods; hence, this section does not apply.